

# Persistent interactions between hydroxylated nanoballs and atactic poly(2-hydroxyethyl methacrylate) (PHEMA)

Kadine Mohamed, Heba Abourahma, Michael J. Zaworotko and Julie P. Harmon\*

Received (in Columbia, MO, USA) 28th February 2005, Accepted 10th May 2005

First published as an Advance Article on the web 27th May 2005

DOI: 10.1039/b503028e

The incorporation of self-assembled nanoparticles, a.k.a. hydroxylated nanoballs, into poly(2-hydroxyethyl methacrylate) (PHEMA) gives rise to a cross-linked network/hydrogel with enhanced interfacial interaction, whereas its inclusion in poly(methyl methacrylate) (PMMA) results in plasticization.

Non-covalent interactions in polymeric systems can arise in a variety of modes, such as hydrogen bonding, electrostatic attractions or  $\pi$ - $\pi$  interactions.<sup>1</sup> Earlier we described the synthesis of a series of metal-organic nanoballs<sup>2</sup> based on the self-assembly of molecular polygons, predisposed to form self-assembled, nanoscale molecules which resemble small rhombihexahedra. The prototypal nanoballs have the formula  $[L_2Cu_2(bdc)_2]_{12}$  (L = solvent or substituted pyridine, bdc = benzene-1,3-dicarboxylate) and are ideally suited for probing polymeric interactions, since they can be functionalized in multiple ways at their surface. For example, groups that may engage in strong hydrogen bonding, e.g. sulfonate, methoxy or hydroxyl, can be positioned on each of the 24 bdc ligands. The axial ligands L can also be substituted. The nature of these nanoballs means that they also have windows that allow access to an internal cavity of volume ca. 1 nm<sup>3</sup>. It was of interest to us to determine if the hydroxylated variant of the nanoball (Fig. 1) would be complementary with poly(2-hydroxyethyl methacrylate) (PHEMA), a hydrogel that we earlier probed with swelling agents.<sup>3</sup> We decided to target PHEMA because of its -OH functionality and because of the possibility that it would form multiple hydrogen bonds with the nanoball and/or become included in its interior. The suprasupermolecular structures<sup>4</sup> that might result from interactions between metal-organic nanoballs and complementary polymer chains would represent a new class of polymer composite, and could potentially be of relevance if the nanoballs were able to fine tune polymer properties, and serve as physical cross-links that were resistant to dissolution.<sup>5</sup>

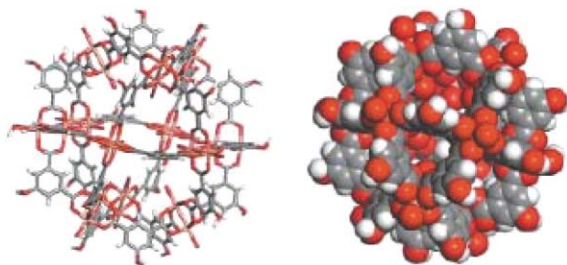


Fig. 1 The crystal structure of  $[(DMSO)(MeOH)Cu_2(bdc-5-OH)_2]_{12}$ .

\*harmon@cas.usf.edu

Hydroxylated nanoballs were prepared as described earlier<sup>2</sup> and dispersed in varying proportions in 2-hydroxyethyl methacrylate (HEMA) and methylmethacrylate (MMA) monomers. The nanoballs were soluble in HEMA, as evidenced by a lack of light scattering (Fig. 2). These solutions were polymerized to form PHEMA nanocomposites that exhibited a high optical transparency between 450–550 nm, presumably due to the excellent dispersion of the nanoballs with minimal or no agglomeration (Fig. 2). The integrity of each individual nanoball was verified by the TEM images shown in Fig. 3. Conversely, the nanoballs did not readily disperse in MMA and a physical dispersive method was needed to break up the agglomerations of nanoparticles. *In situ* ultrasonic polymerization was subsequently employed to fabricate the PMMA nanocomposites.<sup>†</sup>

The glass transition temperatures of the composites were determined using differential scanning calorimetry (DSC).<sup>‡</sup> As revealed in Table 1, the glass transition temperature,  $T_g$ , increased with nanoball concentration in the PHEMA nanocomposites but decreased in the PMMA nanocomposites. The increase in gel fraction of the PHEMA nanocomposites (Table 2) is characteristic of an increase in the cross-linking density of the polymer network. This is directly related to a reduction in the available free volume, resulting in an increase in  $T_g$ .<sup>6</sup> Microhardness data also confirmed the existing trend, in which the hardness number increased with nanoball concentration in the PHEMA nanocomposites. The

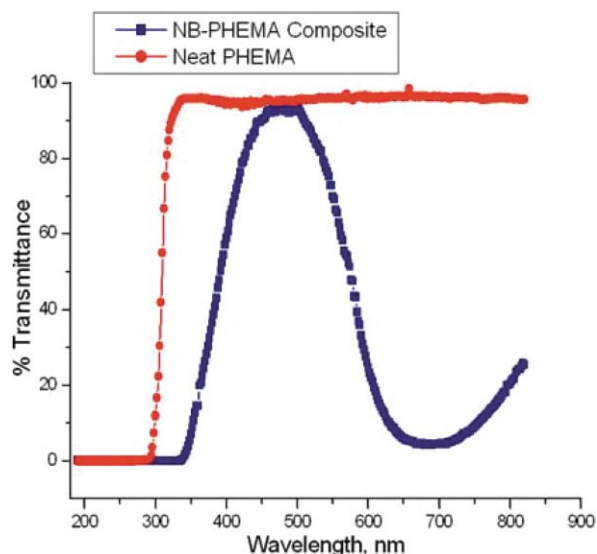
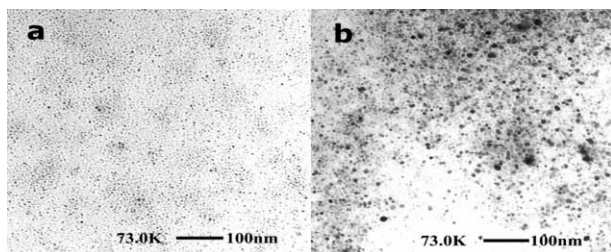


Fig. 2 UV-VIS comparison of neat PHEMA and 1.5% nanoball-PHEMA composite.



**Fig. 3** TEM images of (a) HEMA–nanoball and (b) Methanol–nanoball dispersions.

**Table 1** The glass transition temperatures,  $T_g$  ( $^{\circ}\text{C}$ ), and Vickers Hardness Numbers,  $HV$  ( $\text{kgf mm}^{-2}$ ), of the polymer nanocomposites

Sample <sup>a</sup>	$T_g/^{\circ}\text{C}$	$HV/\text{kgf mm}^{-2}$
Neat PHEMA	99	$24.12 \pm 0.35$
0.1% NB–PHEMA	100	$28.23 \pm 0.21$
0.5% NB–PHEMA	101	$30.03 \pm 0.32$
0.9% NB–PHEMA	104	$33.20 \pm 0.12$
Neat PMMA	113	$31.13 \pm 0.84$
0.05% NB–PMMA	109	$24.74 \pm 0.56$
0.1% NB–PMMA	108	$23.68 \pm 0.35$

<sup>a</sup> NB = nanoball.

**Table 2** Gel fraction of NB–PHEMA nanocomposites

Sample	Gel fraction
Neat PHEMA	$0.82 \pm 0.02$
0.1% NB–PHEMA	$0.84 \pm 0.01$
0.5% NB–PHEMA	$0.91 \pm 0.01$
0.9% NB–PHEMA	$0.94 \pm 0.02$

hardness of a material is a measure of its resistance to surface deformation.<sup>7,8</sup> The increased resistance to surface deformation of the PHEMA nanocomposites may be due to the decreasing free volume content of the matrix, associated with the apparent physical cross-linking and/or entanglements taking place.<sup>9</sup> In contrast, the opposite effect was observed in the PMMA nanocomposites, in which the nanoball appeared to act as a plasticizer. The decrease in  $T_g$  is indicative of an increase in the free volume available in the matrix. When a load is applied to the surface, as in microindentation experiments, the polymer chains are able to slide past each other more easily, resulting in a decrease in the surface hardness number.<sup>10</sup> Dielectric analysis (DEA) of the nanocomposites further confirmed this behaviour. Dielectric analysis was used to determine the molecular motions and structural relaxations present in the composites; it also revealed the mobility of ions, or ionic conductivity, through the polymer matrix.

The PHEMA nanocomposites exhibited a decrease in ionic conductivity and an increase in ionic conductivity activation energy as the nanoball concentration was increased. For example, the ionic conductivities/activation energies for neat PHEMA and 0.9% PHEMA nanocomposite are  $1.95 \times 10^{-5} \text{ S m}^{-1}/35 \text{ kJ mol}^{-1}$  and  $3.38 \times 10^{-6} \text{ S m}^{-1}/45 \text{ kJ mol}^{-1}$  respectively. This was due to the immobilization of the matrix by nanoball interaction. PMMA nanocomposites consistently showed the opposite effect, in which there was an increase in the ionic conductivity and a decrease in the ionic conductivity activation energy as the nanoball

concentration was increased. This indicates the matrix motion was enhanced by the nanoball “plasticizer”.

The data suggest that there is a cross-linking effect taking place in the PHEMA nanocomposites in which there is enhanced nanoball–polymer interaction. An attempt was made to remove the nanoballs from the PHEMA matrix by Soxhlet extraction in methanol. After more than 1 week in the apparatus, no nanoballs were detected in the solvent. In contrast, the DSC and DEA data derived for the PMMA nanocomposites indicated that there was minimal interaction between the nanoball and the matrix, resulting in plasticization. Consequently the nanoballs were easily removed from the PMMA matrix by Soxhlet extraction. The *in situ* ultrasonic polymerization technique developed in our laboratory for the PMMA system produced samples that were optically transparent but still containing nanoagglomerates.

In summary, the PHEMA–nanoball nanocomposites exhibit what appear to be physical cross-links; whereas nanoballs plasticize the PMMA matrix. These encouraging results spur us to further probe these nanoball–polymer systems to further enhance our understanding of the persistent interaction observed in this study. We are currently investigating the interactions of hydroxylated nanoballs with linear PHEMA, as well as the interaction of non-hydroxylated nanoballs with various polymer matrices. Understanding these interactions will give us the capability to fine tune the end properties of inorganic–organic supramolecular compounds.

We thank Krystal McCann and Ed Haller for the TEM images. We gratefully acknowledge the financial support of NSF (DMR-0101641).

**Kadine Mohamed, Heba Abourahma, Michael J. Zaworotko and Julie P. Harmon\***

*Department of Chemistry (SCA 400), University of South Florida, 4202 E. Fowler Avenue, Tampa, FL 33620, USA.*

*E-mail: harmon@cas.usf.edu; Fax: +1 (813) 974 3203;*

*Tel: +1 (813) 974 3397*

## Notes and references

† (1) Synthesis of PHEMA–nanoball nanocomposite: HEMA monomer was obtained from Benz R&D (Sarasota, FL). 0.2 wt% of the free radical initiator 2,2'-azobis(2,4-dimethylvaleronitrile) (Vazo52<sup>®</sup>, DuPont) was added to the monomer, de-gassed with dry  $\text{N}_2$  and polymerized at  $60^{\circ}\text{C}$  for 6 h, followed by a post-cure session at  $110^{\circ}\text{C}$  for 4 h. Various concentrations by wt% of the nanocomposite were prepared by dissolving the nanoballs in HEMA monomer prior to polymerization. It should be noted that the monomer contained a small amount of dimethacrylate impurity, which resulted in the cross-linking of the polymer. (2) Synthesis of PMMA–nanoball nanocomposite: The nanoballs have minimal affinity for methyl methacrylate and were dispersed throughout the matrix by *in situ* ultrasonic polymerization using a Branson Sonifier 450 probe. The monomer and nanoballs were sonicated in an ice bath under a nitrogen atmosphere for 1 h. 0.2 wt% of Vazo52<sup>®</sup> was added and the mixture sonicated under a nitrogen atmosphere in an oil bath at  $80^{\circ}\text{C}$  until the mixture became viscous. The sonifier probe was removed and polymerization allowed to continue in the heated bath for 24 h. The samples were post-cured at  $120^{\circ}\text{C}$  for 4 h.

‡ Instrumentation and characterization: Experiments were performed on a TA Instruments DSC 2920 to determine the glass transition temperature,  $T_g$ . Samples (4–10 mg) were hermetically sealed in aluminium pans and a heat–cool–heat cycle performed. The DSC's cell, which was calibrated with indium and kept under an inert nitrogen atmosphere, was heated using a ramp rate of  $10^{\circ}\text{C min}^{-1}$  to  $140^{\circ}\text{C}$ , quench cooled with liquid nitrogen and then reheated at the same rate. The  $T_g$  was taken from the second heating cycle. Dielectric analysis was performed using a TA Instruments DEA 2970. The sample was heated to  $140^{\circ}\text{C}$  and then taken down to

cryogenic temperatures using liquid nitrogen. A maximum force of 250 N was applied to the sample to achieve a minimum spacing of 0.25 mm. Measurements were taken in 5 °C increments from -150 to 200 °C, in the frequency range 0.1–100 kHz, under a dry nitrogen atmospheric purge of 500 ml min<sup>-1</sup>. Capacitance and conductance were measured as a function of time, temperature and frequency to obtain the dielectric constant, or permittivity ( $\epsilon'$ ) and the dielectric loss ( $\epsilon''$ ). A Leica VMHT MOT equipped with a square Vickers indenter was used to perform microindentation. The Vickers Hardness Number, *HV*, for each sample was determined at room temperature. Values were taken as the average of 5 indents. A load of 500 g and dwell time of 10 s were used. Each sample was approximately 1 mm thick. Gel fractions were obtained by Soxhlet extraction, using methanol as the solvent. An Agilent Technologies 8453 UV-VIS diode array spectrometer was used to determine optical transparency and a Philips CM10 TEM used to obtain micrographs.

- 1 A. F. M. Kilbinger and R. H. Grubbs, *Angew. Chem., Int. Ed.*, 2002, **41**, 1563–1566.
- 2 H. Abourahma, A. W. Coleman, B. Moulton, B. Rather, P. Shahgaldian and M. J. Zaworotko, *Chem. Commun.*, 2001, 22, 2380–2381; B. Moulton, J. Lu, A. Monda and M. J. Zaworotko, *Chem. Commun.*, 2001, 9, 863–864.
- 3 G. Gates, J. P. Harmon, J. Ors and P. Benz, *Polymer*, 2003, **44**, 207–214; G. Gates, J. P. Harmon, J. Ors and P. Benz, *Polymer*, 2003, **44**, 215–222.
- 4 U. S. Schubert, C. H. Weidl, A. Cattani, C. Esch-Baumer, G. R. Newkome, E. He, E. Harth and K. Mullen, *Polymer Prepr. (Am. Chem. Soc., Div. Polym. Chem.)*, 2001, **41**, 229–230.
- 5 K. Nam, J. Watanabe and K. Ishihara, *Eur. J. Pharm. Sci.*, 2004, **23**, 261–270.
- 6 U. W. Gedde, *Polymer Physics*, Chapman and Hall, New York, 1995.
- 7 M. P. Stevens, *Polymer Chemistry: An Introduction*, Oxford University Press, New York, 2nd edn., 1990.
- 8 *Hardness Testing*, ed. H. Chandler, ASM International, Materials Park, Ohio, 2nd edn., 1999, ch. 1, pp. 1–14.
- 9 O. N. Tretinnikov, S.-I. Fujita, S. Ogata and Y. Ikada, *J. Polym. Sci., Part B: Polym. Phys.*, 1999, **37**, 1503–1512.
- 10 V. Lorenzo, R. Benavente, E. Pérez, A. Bello and J. M. Pereña, *J. Appl. Polym. Sci.*, 1993, **48**, 1177–1181.